Asian Journal of Current Research in Clinical Cancer
ISSN: 3062-4444
2022, Volume 2, Issue 1, Page No: 84-100

Available online at: www.galaxypub.co/page/journals

Galaxy Publication

Galaxy Publication

Optimization and Clinical-Scale Production of GMP-Grade NK Cells for Adoptive Cancer Immunotherapy

P. Davies[1*], S. Johnson[1], R. Miller[1]

[1]Department of Clinical Oncology, School of Medicine, University of Queensland, Brisbane, Australia.

***E-mail** ✉ uq.clinical.11@emailprovider.net

Received: 12 January 2022; **Revised:** 10 March 2022; **Accepted:** 11 March 2022

ABSTRACT

Natural killer (NK) cells are a promising avenue for cancer immunotherapy, but efficient clinical-scale production remains challenging. Here, we present an optimized protocol for the activation and expansion of NK cells (NKAE) and its validation under clinical-grade conditions. NK cells were expanded from either total peripheral blood mononuclear cells (PBMCs) or CD45RA+ subsets using irradiated K562 feeder cells expressing IL15-41BBL or IL21-41BBL, with culture media including RPMI-1640, SCGM, NK MACS, and TexMACS. Expansion rate, purity, activation markers, cytotoxic function, and transcriptomic changes were evaluated. Clinical-grade NKAE cells were produced using the CliniMACS Prodigy system. NK MACS and TexMACS media provided superior NK cell purity and minimal T cell contamination. While NKAE generation from CD45RA+ cells was feasible, PBMCs offered higher cell yield and purity. The greatest expansion and purity were achieved with PBMCs stimulated by K562mbIL21-41BBL, though activation status and cytotoxicity were similar across all conditions. Transcriptomic profiling revealed marked differences between resting NK cells and NKAE cells expanded with either IL15- or IL21-expressing feeders. All clinical-grade NKAE preparations met regulatory quality criteria. Our findings demonstrate that GMP-compliant NK cells suitable for immunotherapy can be efficiently expanded using different starting cell populations and feeder strategies, supporting their use in clinical applications.

Keywords: NK cell therapy, NK cell activation and expansion, Clinical-grade NK cells, CliniMACS Prodigy, Immunotherapy

How to Cite This Article: Davies P, Johnson S, Miller R. Optimization and Clinical-Scale Production of GMP-Grade NK Cells for Adoptive Cancer Immunotherapy. Asian J Curr Res Clin Cancer. 2022;2(1):84-100. https://doi.org/10.51847/0mz81D1ojH

Introduction

Developing donor lymphocyte infusion products with potent antitumor activity while minimizing the risk of graft-versus-host disease (GvHD) remains a key challenge in cancer immunotherapy. Natural killer (NK) cells, as innate immune lymphocytes, can detect and eliminate tumor cells without prior sensitization, making them attractive candidates for cellular therapies [1]. NK cell infusions are generally well tolerated, do not trigger GvHD or autoimmune reactions, and have been linked to complete remission in high-risk acute myeloid leukemia (AML) patients [2, 3].

A major limitation in NK cell therapy is that effective clinical outcomes require both sufficient cell numbers and high activation status, yet these parameters are often low in standard NK cell sources, such as peripheral blood mononuclear cells (PBMCs) or umbilical cord blood units. To address this, various ex vivo expansion and activation protocols have been developed. These approaches differ in their cytokine supplementation [4–7], the NK cell source utilized [8, 9], or the type of feeder or artificial antigen-presenting cells (aAPCs) employed [10–12]. Despite these variations, expanded and activated NK cells (NKAE) typically share enhanced activation markers and cytotoxic activity, including the ability to kill tumor targets resistant to resting NK cells [10, 13–15]. Several groups have engineered K562 feeder cells to express membrane-bound interleukin-15 (mIL-15) or IL-21 along with CD137 ligand (4-1BBL). These feeder cells provide synergistic activating signals, co-stimulation, and survival cues via cytokines, promoting the proliferation of highly cytotoxic NK cells [11, 12].

Translating these protocols to a clinical scale under good manufacturing practice (GMP) conditions remains complex. Manual scale-up involves multiple labor-intensive steps, limiting routine application. The CliniMACS Prodigy platform from Miltenyi Biotec allows automated, closed-system production using centrifugation, magnetic separation, and cell cultivation [16]. Several groups have leveraged this system to establish reproducible NK cell expansion protocols suitable for clinical use [17–19].

Additionally, selective T-cell depletion in allogeneic hematopoietic stem cell transplantation (HSCT) grafts is evolving. Depletion of the CD45RA+ naive T-cell subset can reduce GvHD, while this fraction, typically discarded, also contains NK cells that could serve as starting material for ex vivo NK cell expansion [20].

The aim of this study was to refine an NK cell activation and expansion protocol by evaluating different culture media, aAPCs, and starting cell populations. Optimized protocols were then validated on the CliniMACS Prodigy system to generate clinical-grade NKAE cells suitable for immunotherapy. Our results demonstrate that automated GMP-compliant NK cell production is achievable, with final products meeting the quality standards set by the Spanish Regulatory Agency.

Results and Discussion

Optimization of cell culture media

NK cell expansion and purity across different media

To evaluate the effect of different culture media on NK cell proliferation and purity, we conducted 21 independent expansion experiments using buffy coat samples from five healthy donors. PBMCs were co-cultured with irradiated K562-mbIL15-41BBL (K562mbIL15) cells at a 1:1.5 ratio in four media: RPMI, Stem Cell Growth Medium (SCGM), NK MACS, and TexMACS GMP, all supplemented with 5% human AB serum and IL-2.

After 21 days, the fold expansion of both total and NK cells was assessed **(Figure 1)**. Although differences were not statistically significant, NK MACS achieved the highest NK cell fold increase (903 ± 576.3), whereas RPMI produced the lowest expansion (388 ± 292.7) ($p = 0.45$).

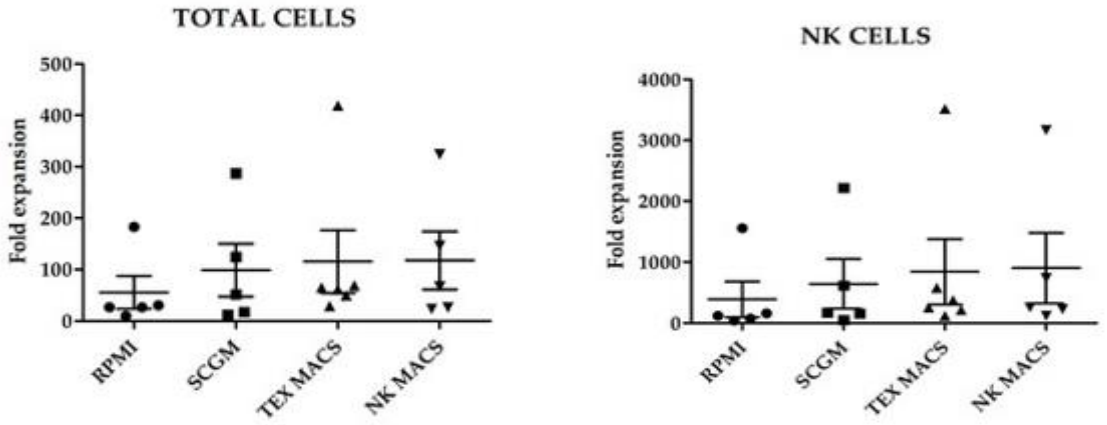

a) b)

Figure 1. Fold expansion of total and NK cells after 21 days of culture in different media. Error bars represent mean ± SEM. For RPMI, SCGM, and NK MACS, n = 5; for TexMACS, n = 6. Each geometric symbol represents the expansion data from an individual donor: RPMI (dots), SCGM (squares), TexMACS (triangles), and NK MACS (inverted triangles).

In terms of NK cell purity, TexMACS GMP achieved the highest proportion of NK cells at day 21 (92.93% ± 2.8%), followed closely by NK MACS (91.75% ± 1.82%), with no statistically significant difference between the two. SCGM resulted in intermediate NK cell purity (81.79% ± 4.05%), whereas RPMI produced the lowest purity (72.97% ± 3.6%), which was significantly lower than TexMACS ($p < 0.05$).

Residual T-cell contamination was lowest in NK MACS (3.5% ± 0.96%) and TexMACS (4.21% ± 2.08%), both lower than SCGM (7.33% ± 2.62%). The highest T-cell presence was observed in RPMI-cultured NKAE cells (10.86% ± 1.47%), although this difference did not reach statistical significance compared to the other media **(Figure 2)**.

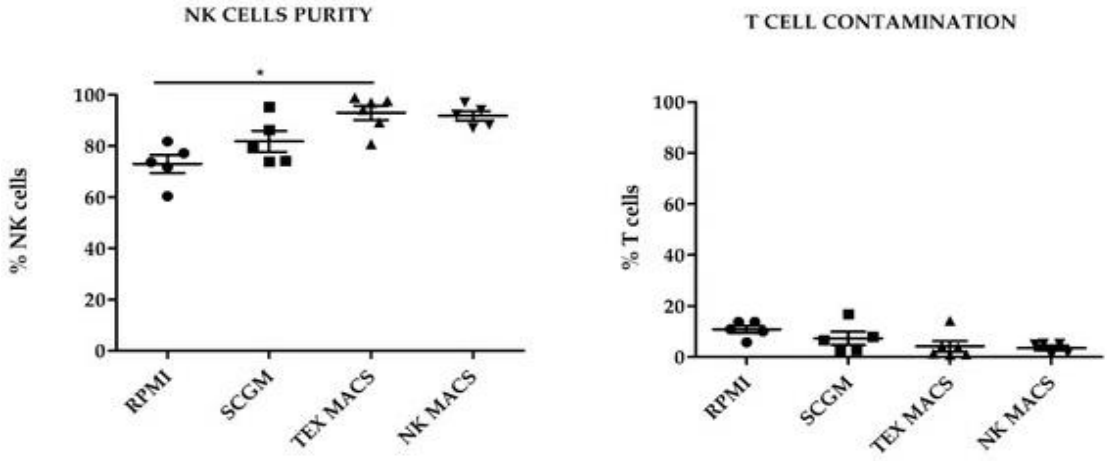

a) b)

Figure 2. NK cell purity and T-cell contamination in NKAE cells expanded using various culture media. Error bars indicate mean ± SEM. Sample sizes: RPMI, SCGM, NK MACS (n = 5); TexMACS (n = 6). *p < 0.05. Each symbol represents data from a different donor: RPMI (dots), SCGM (squares), TexMACS (triangles), NK MACS (inverted triangles).

We also assessed the composition of NK cell subtypes (bright and dim) and overall viability throughout the culture period. Viability remained comparable across all media. Interestingly, RPMI-expanded NKAE cells had a higher proportion of bright NK cells than the other media, which corresponded to a lower proportion of dim NK cells; statistical significance was reached only in comparison to TexMACS. No meaningful differences were observed in the proportions of NKT or B cells after 21 days of culture.

Phenotypic analysis of NKAE cells

Flow cytometry was used to evaluate NKAE cells at the start of culture and after 21 days of expansion with K562mbIL15 cells in RPMI, SCGM, NK MACS, or TexMACS. All culture conditions led to increased surface expression of key activating receptors (CD25, CD69, NKG2D, NKp30, NKp44, NKp46, and DNAM-1) relative to resting NK cells. Significant differences were observed only for NKG2A and NKp46: NKG2A expression was elevated in NKAE cells expanded in TexMACS ($p = 0.01$), while NKp46 was significantly higher in RPMI-expanded NKAE cells ($p = 0.013$) compared with baseline levels **(Figure 3)**.

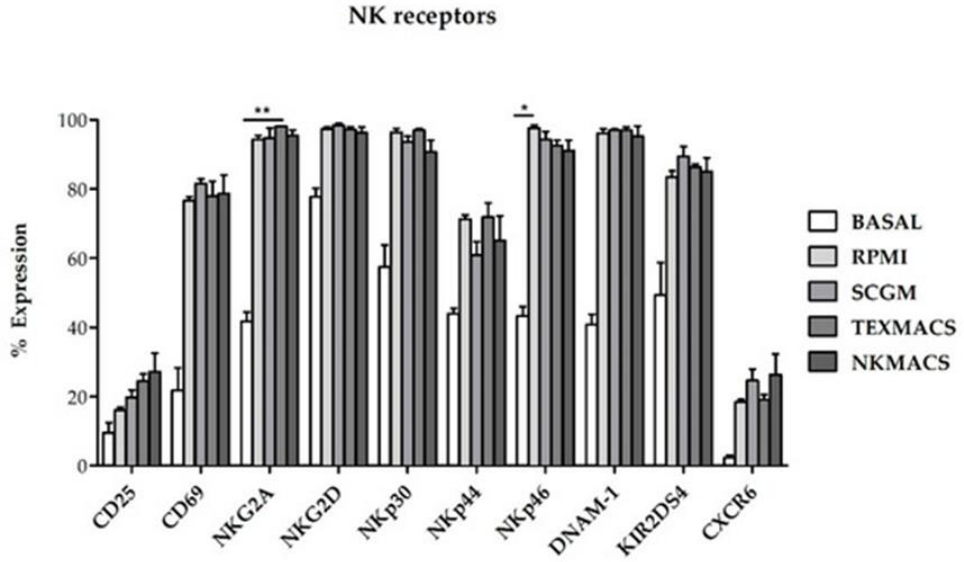

Figure 3. Surface receptor expression on NKAE cells expanded in various culture media. The levels of activating and inhibitory receptors were elevated in all NKAE cells compared with resting NK cells. No significant differences were observed in receptor expression among NKAE cells expanded in different media. Error bars represent mean ± SEM; n = 3 per condition. (*p = 0.013, **p = 0.01).

Assessment of NKAE cell cytotoxic function

The cytotoxic potential of NKAE cells cultured in the different media was tested against K562 target cells. Across all media conditions, NKAE cells demonstrated comparable lytic activity, with no statistically significant differences detected **(Figure 4)**.

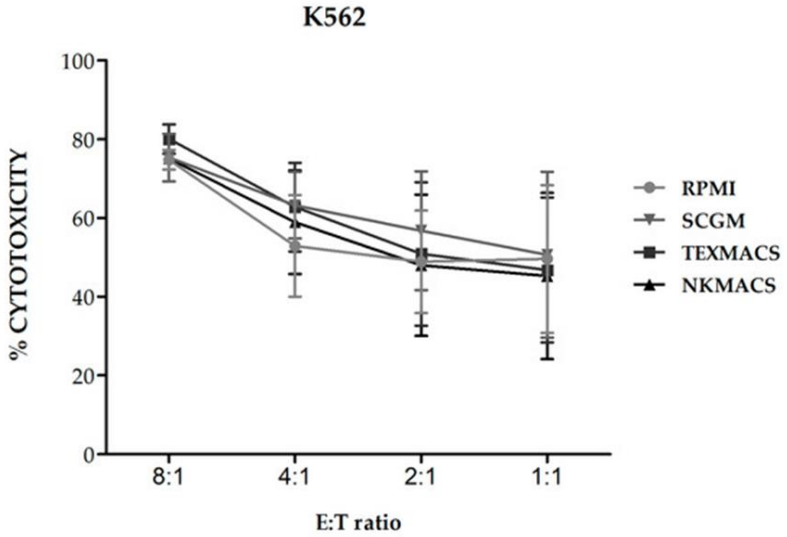

Figure 4. Cytotoxicity of NKAE cells expanded with different culture media against K562 cells. The NKAE cells expanded with the different culture media did not show differences in their cytolytic ability against K562 cells. Error bars show mean ± SEM. n = 3 for each condition.

CD45RA+ cells as a source for NKAE cell expansion

The CD45RA+ fraction contains both naïve T cells and NK cells. In certain hematopoietic stem cell transplantation (HSCT) protocols, this fraction is removed to eliminate alloreactive T cells and thereby reduce the risk of graft-versus-host disease (GvHD). In contrast, the CD45RA– memory T cell population lacks naïve T cells and exhibits lower alloreactivity, which supports engraftment and provides protection against infections. CD45RA– cells can be administered to patients undergoing haploHSCT either within the graft alongside mobilized CD34+ cells or as donor lymphocyte infusions (DLI). Typically, CD45RA– grafts are derived from healthy donors following pharmacologic stem cell mobilization with G-CSF [21], though some approaches utilize non-mobilized apheresis [22]. Likewise, CD45RA+ fractions intended for DLI are obtained from non-mobilized apheresis [23].

To investigate whether NK cells could be efficiently expanded from the CD45RA+ “waste” fraction, we performed ex vivo expansions using CD45RA+ cells collected from both mobilized and non-mobilized apheresis and compared the outcomes with expansions starting from total PBMCs. Based on previous optimization experiments, TexMACS medium was selected for these expansions. The initial composition of the cell products prior to culture is illustrated in **Figure 5**. CD45RA+ cells from mobilized apheresis displayed the lowest baseline NK cell percentage (1.7% ± 0.6%), followed by CD45RA+ cells from non-mobilized apheresis (7.5% ± 2.5%), while PBMCs had the highest starting NK cell content (16.9% ± 2.7%).

After 21 days of culture, the fold expansion of NK, NKT, T, and B cells was assessed **(Figure 6)**. The CD45RA+ mobilized fraction exhibited the lowest NK cell expansion (7.6 ± 4.2-fold; $p = 0.011$ vs. PBMCs) and the highest expansion of B cells (306.3 ± 79.9-fold; $p = 0.014$ vs. PBMCs).

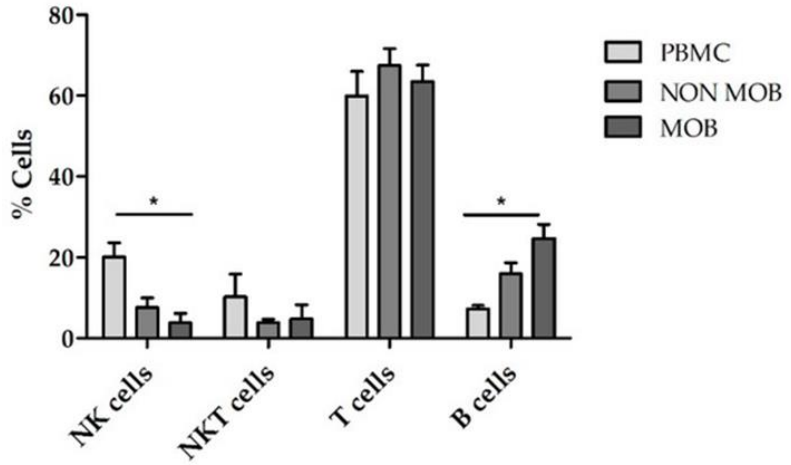

Figure 5. Cell subsets contained in PBMC, CD45RA$^+$ cells from mobilized apheresis (mob) and CD45RA$^+$ cells from non-mobilized apheresis (non-mob) before NK cell expansion. Mobilized CD45RA$^+$ cells contain less NK and more B cells compared to PBMC $p = 0.03$ and $p = 0.01$ respectively. PBMC (n = 5), non-mob (n = 3) and mob (n = 3). Error bars show mean ± SEM. * $p < 0.05$.

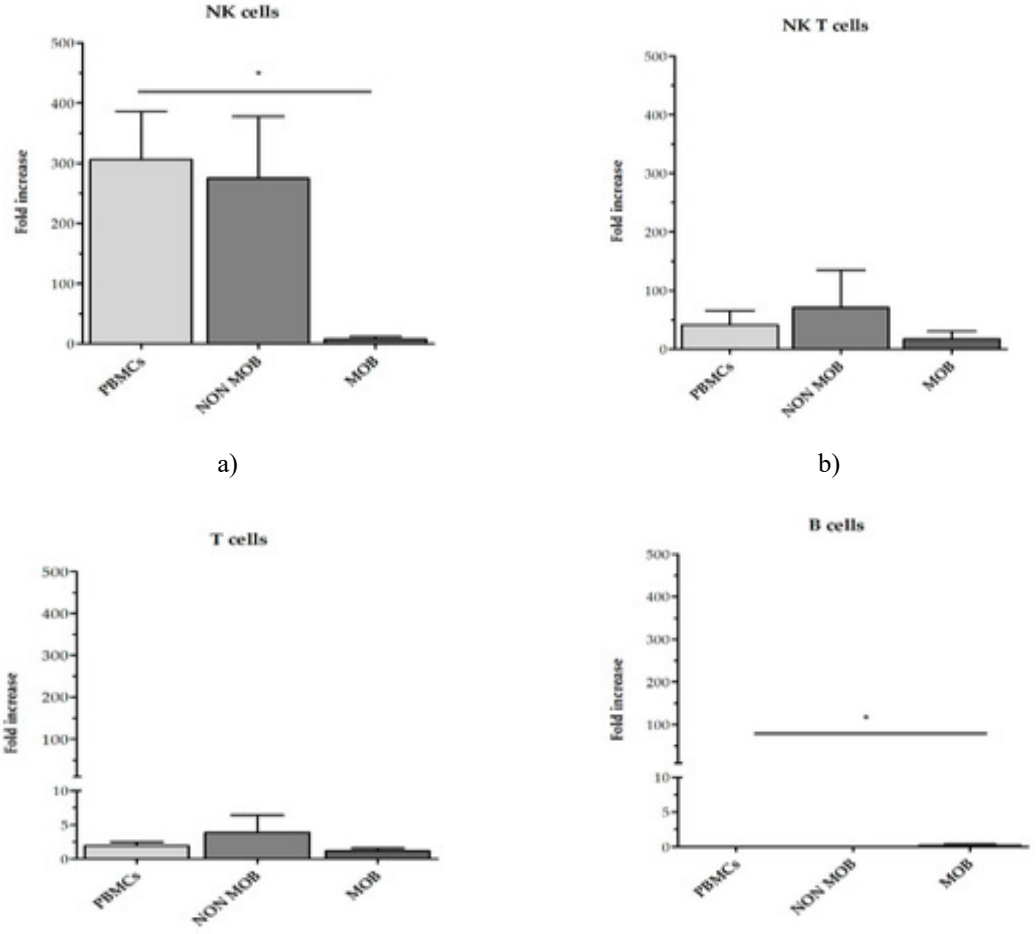

Figure 6. Fold expansion of various cell subsets within NKAE populations generated from PBMCs, CD45RA$^+$ mobilized apheresis, and CD45RA$^+$ non-mobilized apheresis on day 21. NKAE cells derived from mobilized apheresis contained fewer NK cells at the end of the culture period compared with those expanded from PBMCs or non-mobilized apheresis. Sample sizes were PBMC (n = 5), non-mobilized (n = 3), and mobilized (n = 3). Data are presented as mean ± SEM. *$p < 0.05$.

Expansion of NKAE cells using different aAPCs

After identifying the optimal culture medium and confirming that NK cells could be successfully expanded from the CD45RA$^+$ fraction, we next assessed whether the aAPC used—either K562-mbIL15 or K562-mb21-41BBL (hereafter referred to as K562-mbIL21)—influenced NKAE cell expansion. NK cells from six donors were expanded for 21 days using either PBMCs or CD45RA$^+$ cells as the starting population and TexMACS as the culture medium. At day 21, we quantified total cell expansion, NK cell purity, cytotoxic activity against four pediatric tumor cell lines (A673, RH30, Jurkat, LAN-1), and against K562 cells as a control.

Cultures initiated with PBMCs generally produced greater total cell numbers and higher NK cell purity compared with those starting from CD45RA$^+$ cells ($2.34 \times 10^8 \pm 5.04 \times 10^7$ vs. $1.08 \times 10^8 \pm 4.38 \times 10^7$; $p = 0.004$) and (72.26% ± 25.54% vs. 65.06% ± 22.68%; $p = 0.015$), respectively. Using PBMCs as input, expansion with K562-mbIL21 resulted in significantly higher total cell output than expansion with K562-mbIL15 ($3.36 \times 10^8 \pm 6.63 \times 10^7$ vs. $1.30 \times 10^8 \pm 5.03 \times 10^7$; $p = 0.03$) and showed a trend toward greater NK cell purity (84.67% ± 4.82% vs. 59.85% ± 12.42%; $p = 0.09$).

When CD45RA$^+$ cells served as the starting material, cultures stimulated with K562-mbIL21 tended to generate more cells ($7.31 \times 10^7 \pm 2.18 \times 10^7$ vs. $1.32 \times 10^8 \pm 8.7 \times 10^7$) and higher NK purity (73.91% ± 5.82% vs. 56.20% ± 11.11%) than those stimulated with K562-mbIL15, although these differences did not reach statistical significance ($p = 0.53$ and $p = 0.19$, respectively).

Overall, NKAE cells expanded with K562-mbIL15 consistently produced fewer total cells ($1.02 \times 10^8 \pm 2.75 \times 10^7$ vs. $2.34 \times 10^8 \pm 6.07 \times 10^7$; $p = 0.023$) and exhibited lower NK cell purity (58.03% ± 7.97% vs. 79.29% ± 3.95%; $p = 0.003$) than those expanded with K562-mbIL21, regardless of whether PBMCs or CD45RA$^+$ cells were used as the initial source **(Figure 7)**.

Flow cytometry assessments throughout the expansion period and at day 21 **(Figure 8)** demonstrated comparable surface marker and receptor expression profiles across all NKAE products, independent of input material or aAPC type. In line with this, NKAE cells derived from all conditions displayed comparable cytotoxic activity against the five tumor cell lines tested **(Figure 9)**.

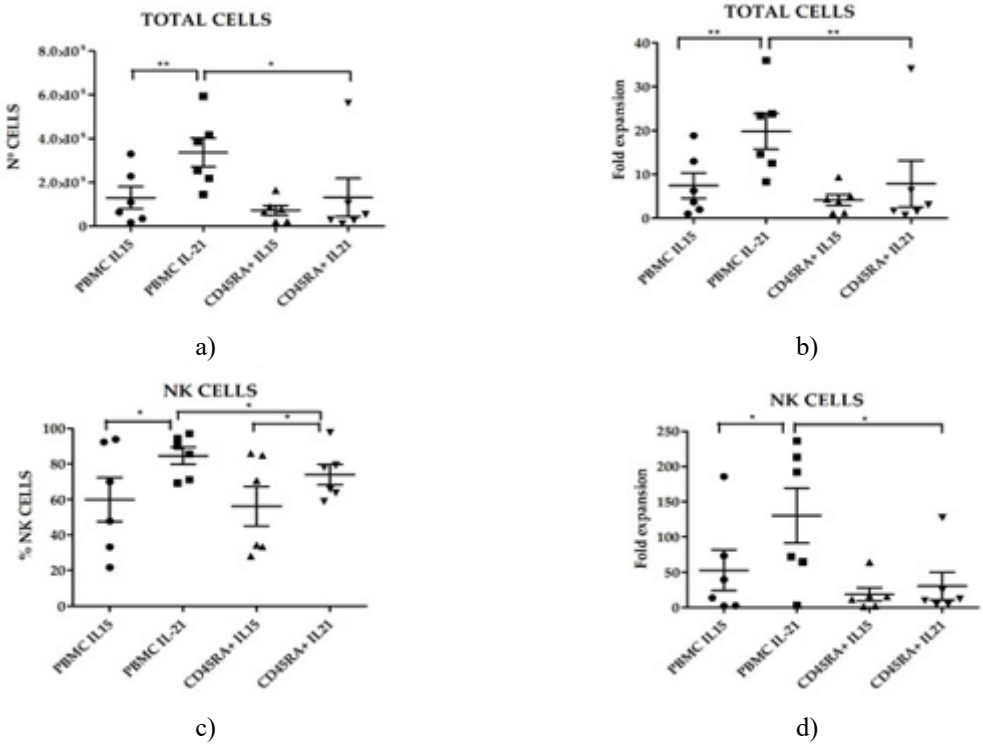

Figure 7. Total cell counts, NK cell purity, and fold expansion of both total cells and NKAE cells using different NK cell sources and artificial antigen-presenting cells (aAPCs) (n = 6 per condition). Data are shown as mean ± SEM. *p < 0.05, **p < 0.01. Geometric symbols indicate individual donor-derived NKAE samples for each condition shown on the X-axis: circles = PBMC + K562-mbIL15; squares = PBMC + K562-mbIL21; triangles = CD45RA$^+$ + K562-mbIL15; inverted triangles = CD45RA$^+$ + K562-mbIL21.

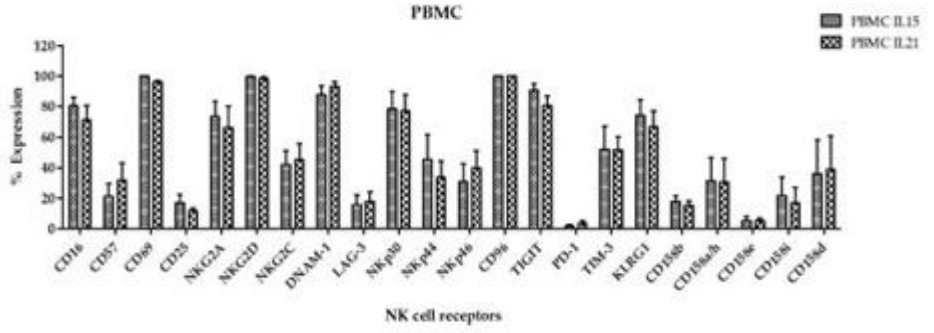

a)

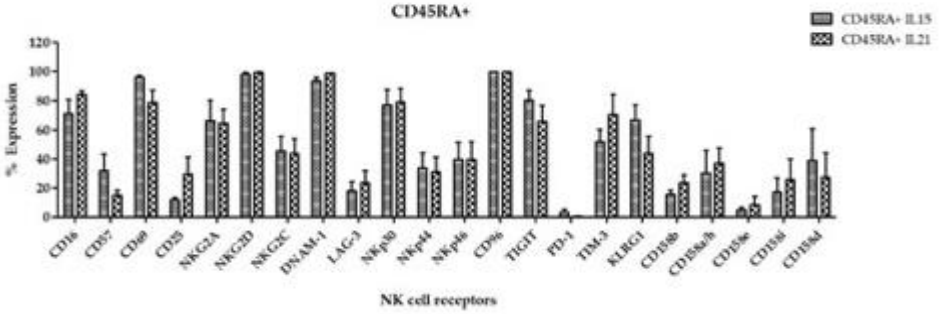

b)

Figure 8. Surface expression of various NK cell receptors on NKAE cells expanded from PBMCs or CD45RA$^+$ cells using K562-mbIL15 or K562-mbIL21 as the aAPC. No significant differences in receptor expression were observed among conditions (n = 4 per group). Data are shown as mean ± SEM.

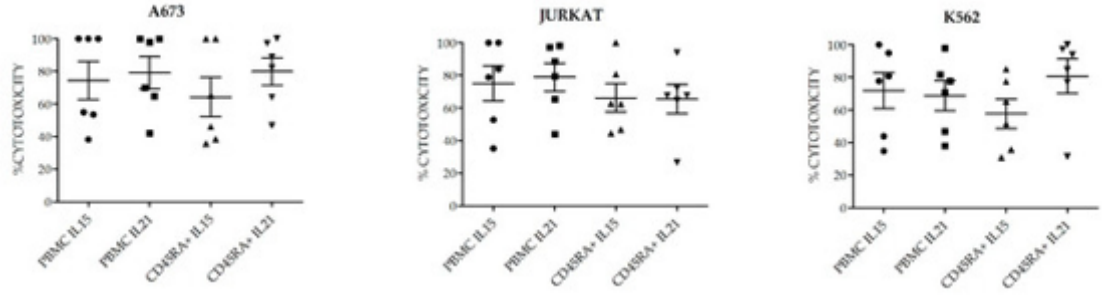

a)

b)

c)

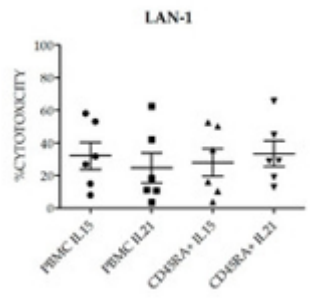

d)

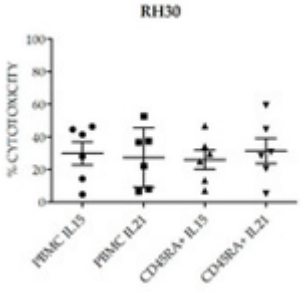

e)

Figure 9. Cytotoxic activity of NKAE cells generated from PBMCs or CD45RA$^+$ cells with K562-mbIL15 or K562-mbIL21 stimulation. NKAE products demonstrated comparable antitumor activity across all conditions. Data are shown as mean ± SEM at an effector-to-target (E:T) ratio of 2:1. Geometric symbols represent individual donor data corresponding to the X-axis conditions: circles = PBMC + K562-mbIL15; squares = PBMC + K562-mbIL21; triangles = CD45RA$^+$ + K562-mbIL15; inverted triangles = CD45RA$^+$ + K562-mbIL21.

Transcriptome analysis of basal NK cells and NKAE products

To investigate gene expression differences between basal NK cells derived from PBMCs or CD45RA$^+$ cells and their corresponding NKAE products expanded with K562-mbIL15 or K562-mbIL21, RNA-seq was performed on samples from two representative donors.

Unsupervised hierarchical clustering of the 15,919 filtered genes separated samples into two major clusters: basal NK cells and NKAE products **(Figure 10a)**. Within the NKAE group, samples further segregated according to stimulation with IL21 or IL15. However, NKAE cells derived from PBMCs or CD45RA$^+$ cells did not form distinct subclusters. A total of 2,185 differentially expressed genes (DEGs) were identified between unstimulated and expanded NK cells. Among these DEGs, 1,178 genes were upregulated and 1,007 were downregulated in stimulated NK cells, using a false discovery rate (FDR) of 0.05 and a log fold-change threshold of 2 **(Figure 10b)**. KEGG pathway enrichment analysis revealed 30 pathways associated with the DEGs, predominantly those involved in cellular growth, apoptosis, and metabolic processes (e.g., cell cycle, hematopoietic lineage development, p53 signaling, pyrimidine metabolism) **(Table 1)**. Gene ontology (GO) classification showed that upregulated genes were enriched in processes such as DNA replication, cell division, and cell proliferation, while downregulated genes were primarily related to cell adhesion and migration.

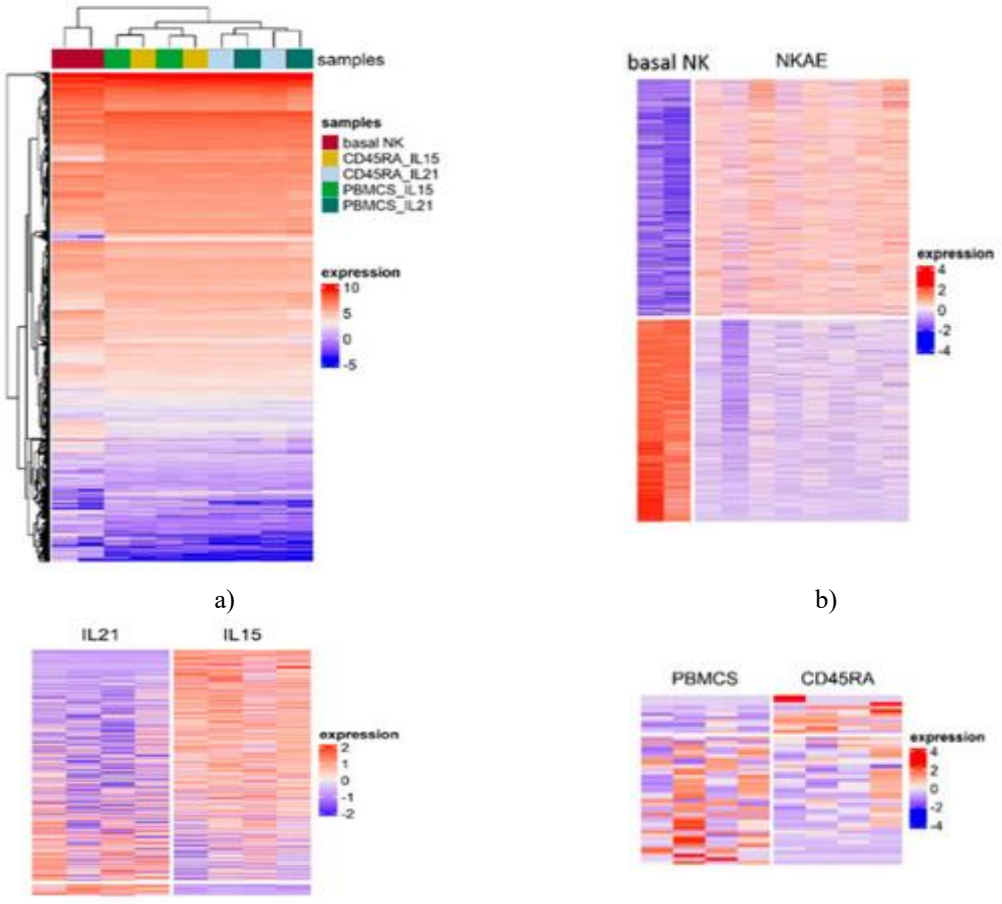

Figure 10. Gene expression patterns in basal NK cells and NKAE products.
(a) Unsupervised hierarchical clustering based on the 15,919 genes that remained after filtering.
(b) Heatmap displaying normalized expression levels of the 2,185 genes differentially expressed between basal NK cells and NKAE products.
(c) Heatmap showing normalized expression values for the 609 genes differentially expressed between IL21- and IL15-stimulated NKAE cells.
(d) Heatmap of the 48 genes differentially expressed between NKAE cells derived from PBMCs and those generated from CD45RA$^+$ cells.

Heatmap colors reflect relative gene expression, with red indicating higher expression and blue indicating lower expression. Each row corresponds to a single gene, and each column represents an individual sample. Color-coded lines mark the sample types: deep red = basal NK cells; green = IL15-stimulated PBMC-derived NKAE cells; yellow = IL15-stimulated CD45RA$^+$-derived NKAE cells; light blue = IL21-stimulated CD45RA$^+$-derived NKAE cells; and emerald green = IL21-stimulated PBMC-derived NKAE cells.

Table 1. KEGG pathways enrichment analysis by differentially expressed genes (DEGs).

Comparison	Total DEGs (Up-regulated + Down-regulated)	KEGG Enriched Pathways (Significant)
NKAE vs. basal NK cells	2185 (1178 ↑ + 1107 ↓)	Cell cycle, Cytokine–cytokine receptor interaction, Viral protein interaction with cytokine and cytokine receptor, Hematopoietic cell lineage, p53 signaling pathway, Cell adhesion molecules (CAMs), Inflammatory bowel disease (IBD), Pyrimidine metabolism, Transcriptional misregulation in cancer, Biosynthesis of amino acids, Glycine, serine and threonine metabolism, Prostate cancer, PI3K-Akt signaling pathway, Antifolate resistance, Asthma, Small cell lung cancer, MAPK signaling pathway, Oocyte meiosis, Human T-cell leukemia virus 1 infection, Chemokine signaling pathway, Leishmaniasis, Cellular senescence, Starch and sucrose metabolism, Tryptophan metabolism, One carbon pool by folate, Carbon metabolism, Glioma, JAK-STAT signaling pathway, Melanoma, HIF-1 signaling pathway
IL21 vs. IL15-stimulated NKAE cells	609 (29 ↑ + 580 ↓)	Cytokine–cytokine receptor interaction, Hematopoietic cell lineage, Asthma, Inflammatory bowel disease (IBD), Primary immunodeficiency, IL-17 signaling pathway, Viral protein interaction with cytokine and cytokine receptor, Leishmaniasis, Fc epsilon RI signaling pathway, Osteoclast differentiation, Transcriptional misregulation in cancer, Rheumatoid arthritis, Protein digestion and absorption, Chemokine signaling pathway, T cell receptor signaling pathway, Th17 cell differentiation, JAK-STAT signaling pathway, Arachidonic acid metabolism, Malaria, NF-kappa B signaling pathway, Cell adhesion molecules (CAMs), Ether lipid metabolism
PBMC vs. CD45RA$^+$-derived NKAE cells	48 (37 ↑ + 11 ↓)	—

A total of 609 genes were differentially expressed when IL21-expanded NKAE cells were compared with those stimulated by IL15. Of these, only 29 genes were more highly expressed under IL21 stimulation, while 580 showed reduced expression **(Figure 10c)**. The contrast between IL21 and IL15 stimulation produced more DEGs in NKAE cells derived from PBMCs than from CD45RA$^+$ cells (547 vs. 381). Pathway enrichment revealed 22 pathways primarily linked to immune and inflammatory mechanisms—such as cytokine–receptor networks, hematopoietic differentiation, IL-17 signaling, and pathways associated with asthma, IBD, and primary immunodeficiency **(Table 1)**. GO analysis highlighted enrichment in processes connected to inflammation, general immune activity, complement activation, B-cell signaling, phagocytosis, and adhesion.

A wide range of cytokines and receptors involved in immune cell activation were expressed at higher levels in IL15-stimulated NKAE cells compared with those expanded using IL21. These included several T- and B-cell–associated markers (e.g., CD4, CD8B, CD19, CD20, CD23), myeloid- and lymphoid-related receptors (CD33, CD116, CD123), and inflammatory cytokines (IL1A, IL1B, IL4, IL5). Among NK-specific receptors, only one KIR family member—**KIR2DL3**—differed significantly, showing increased expression under IL21 stimulation. Expression of LIR1, NKG2 family members (A, C, D) and the main NCRs did not differ. The checkpoint receptor **PD-1** was more strongly expressed in IL15-expanded cells. Genes regulating apoptosis or cell-cycle progression showed no meaningful differences between the two stimulation conditions.

When NKAE cells generated from PBMCs were compared with those derived from CD45RA$^+$ cells, only a small gene set differed: 48 DEGs in total (37 upregulated, 11 downregulated in PBMC-derived NKAE cells) **(Figure 10d)**. These genes did not cluster into significant GO or KEGG categories overall. However, under IL21 stimulation specifically, two pathways—hematopoietic lineage development and arachidonic acid metabolism—were enriched in PBMC-derived NKAE cells relative to CD45RA$^+$-derived NKAE cells.

Generation of clinical-grade NKAE cells using the cliniMACS prodigy

After optimizing NK cell expansion parameters, we assessed whether these conditions could be translated into an automated, GMP-compliant manufacturing system. For this purpose, NKAE cells were expanded at clinical scale on the CliniMACS Prodigy® device (Miltenyi Biotec). Non-mobilized apheresis served as the starting product and TexMACS GMP medium was used throughout. To shorten the culture period, the process incorporated GMP-compatible CD3 depletion followed by CD56 enrichment. Irradiated K562-mbIL15 or K562-mbIL21 cells functioned as the aAPCs.

Between 2 and 2.5 × 10^6 purified $CD56^+$ cells were cocultured with approximately 40 × 10^6 irradiated aAPCs (about a 1:20 ratio). Cell viability, expansion, and NK cell frequencies at baseline, and again at days 7 and 14, are summarized in **Table 2**.

Table 2. Characteristics of CD56 starting cells and expanded NKAE cells a day +7 and +14 (end of culture). (*) Viability measured in CD45+ cells. (**) At day 0, analysis was performed in CD56+ cells before coculture with K562mbIL15 cells.

K562mbIL15	**% Viability (*)**	**% NK Cells**	**% T Cells**	**Total Cells**	**Total NK Cells**
Day 0 (**)	96	87	22.8	2.9 × 106	2.5 × 106
Day +7	95	87.1	1	80 × 106	76 × 106
Day +14	97	97.1	1.2	654 × 106	635 × 106
K562mbIL21	**% Viability (*)**	**% NK Cells**	**% T Cells**	**Total Cells**	**Total NK Cells**
Day 0 (**)	96	77	14.8	3.4 × 106	2 × 106
Day +7	99.3	90.7	3.5	107.5 × 106	97.5 × 106
Day +14	97	93	1.6	1498 × 106	1393 × 106

On day 0, before the expansion, both $CD56^+$ cells and aAPC met the acceptance criteria (sterility, mycoplasma negative and viability ≥70%).

At the end of coculture (Day +14), NKAE cells expanded in CliniMACS Prodigy showed an upregulation of all the receptors analyzed **(Figure 11)**.

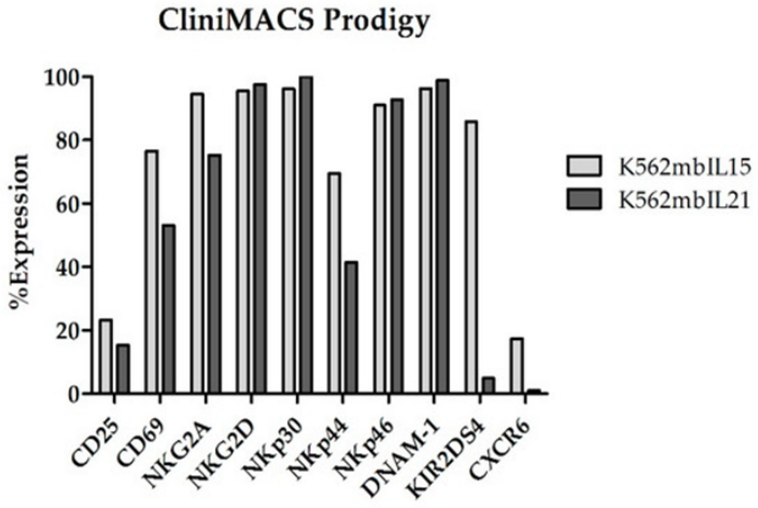

Figure 11. NK cell receptors are upregulated on NKAE cells manufactured in CliniMACs Prodigy.

At the completion of the manufacturing process, NKAE products had to satisfy several release requirements: a minimum viability of 70%, at least 50% cytotoxic activity against K562 targets at an 8:1 effector-to-target ratio, negative mycoplasma testing, sterility confirmed by the absence of colony-forming units, endotoxin levels no higher than 0.25 EU/mL, no detectable bcr/abl transcript indicating removal of residual aAPCs, and no elevated expression of the oncogenic markers C-MYC or TERT. As summarized in **Table 3**, all NKAE batches fulfilled these quality and safety specifications, meeting the criteria necessary for clinical release.

Table 3. The manufactured NKAE cells met the established acceptance criteria.

aAPC	Sterility	Mycoplasma	Endotoxins	c-myc/tert	Bcr/abl	Cytotoxicity
K562mbIL15	0 CFU	Negative	<0.01 EU/mL	No expression	0%	79%
K562mbIL21	0 CFU	Negative	<0.03 EU/mL	No expression	0%	100%

Natural killer (NK) cells possess the intrinsic ability to rapidly eliminate tumor cells and have been evaluated in multiple clinical trials for the treatment of various malignancies [24]. Considerable progress has been achieved in NK-cell–based therapies, both in the context of haploidentical stem cell transplantation (haploSCT) [25–27] and in non-transplant settings [28–30], given that NK cells mediate graft-versus-leukemia/tumor (GvL/GvT) effects without inducing graft-versus-host disease (GvHD) [26, 27, 31].

Despite their therapeutic promise, the clinical implementation of NK cells faces two main challenges: (1) NK cells constitute only a small subset of peripheral blood leukocytes, necessitating substantial expansion to reach clinically meaningful doses, and (2) NK cells must be fully activated to exert robust antitumor activity. Overcoming these barriers requires the development of GMP-compliant, scalable manufacturing strategies. Multiple protocols have been designed to produce activated NK cells for clinical use that differ in their NK-cell source—PBMCs [32], umbilical cord blood [33], or the NK-92 cell line [34]—their use of activating cytokines [7, 35], and the inclusion or exclusion of feeder cell systems [14, 34–36].

The objectives of this study were threefold: (1) to optimize NK-cell activation and expansion at small scale, (2) to evaluate the feasibility of large-scale manufacturing of NKAE cells in a manner compatible with clinical application, and (3) to verify that the final NKAE products fulfilled the release requirements established by the Spanish Regulatory Agency. To identify the optimal culture medium, PBMCs were cocultured with irradiated K562mbIL15 cells in four GMP-compliant media (RPMI, SCGM, TexMACS, NK MACS). Although RPMI yielded slightly lower cell numbers, overall NK-cell and total-cell expansion was comparable among all media. TexMACS and NK MACS produced the highest NK-cell purity with minimal T-cell contamination, making them the preferred options for generating highly pure NKAE products. These data align with findings by Klöß *et al*. [19], who reported superior NK-cell expansion in NK MACS relative to X-VIVO-10, SCGM, or TexMACS, although their results showed a more pronounced difference than observed here. This discrepancy may stem from their use of higher IL-2 concentrations (1000 IU/mL vs. 10–100 IU/mL), different starting populations (purified CD56+CD3– cells), or other methodological differences. The reduced expansion observed in RPMI is consistent with Duck *et al*., who demonstrated improved NK-cell activation and proliferation in SCGM compared with RPMI-1640 [37].

Having established the most suitable culture medium, we next examined whether NKAE cells could be generated from the CD45RA+ cell fraction. CD45RA− cells, enriched in central and effector memory T cells, provide protective immunity against previously encountered antigens and reduce alloreactivity; consequently, they are often infused as donor lymphocyte infusions (DLIs) to reduce GVH risk after HSCT [38]. CD45RA− cells are obtained by depleting CD45RA+ cells—a population enriched in naïve T cells and NK cells—suggesting CD45RA+ cells as a potential NK-cell source. In our study, CD45RA+ cells derived from G-CSF–mobilized apheresis failed to expand, whereas CD45RA+ cells from non-mobilized apheresis expanded comparably to PBMC-derived cultures. These results demonstrate that CD45RA+ cells from non-mobilized donors can serve as an effective NK-cell source. The poor expansion from G-CSF–mobilized collections is consistent with earlier reports showing reduced NK-cell mobilization and cytotoxicity following G-CSF exposure [39, 40]. For future applications requiring cell mobilization, plerixafor may be preferable since it efficiently mobilizes NK cells [41].

We then compared NKAE cells generated from PBMCs and CD45RA+ cells using two aAPCs: irradiated K562mbIL15 and K562mbIL21. PBMC-derived NK cells showed higher fold expansion than those from CD45RA+ cells, independent of the aAPC used. Coculture with K562mbIL21 consistently produced greater total-cell expansion and higher NK-cell purity across NK-cell sources, indicating that PBMCs cocultured with K562mbIL21 represent the most effective strategy for generating large quantities of purified NKAE cells. These findings are in agreement with earlier work by Denman *et al*. [42], who reported that IL-21–expressing K562 feeder cells drive enhanced NK-cell proliferation, potentially due to reduced senescence and longer telomere length in expanded NK cells. Importantly, NKAE products generated from different sources and feeder cells displayed comparable NK-receptor profiles and in-vitro cytotoxicity across multiple tumor targets.

Transcriptomic analysis revealed distinct gene expression signatures between stimulated and unstimulated NK cells, predominantly involving genes associated with cell cycle progression, metabolic activity, and growth.

Several genes with high differential expression—such as UBE2C, TK1, AURKB, RRM2, and FCN1—are known to be upregulated during NK-cell activation and proliferation [11, 43]. A substantial number of DEGs were also detected between IL-21– and IL-15–stimulated NKAE cells, particularly in PBMC-derived cultures. Most DEGs were downregulated in IL-21–expanded NKAE cells, affecting pathways including hematopoietic lineage, chemokine signaling, JAK–STAT, and PI3K–Akt. These differences suggest that IL-21 promotes a more undifferentiated NK-cell phenotype, whereas IL-15 drives a more activated transcriptional program.

Denman *et al*. [42] reported that IL21- and IL15-expanded NK cells exhibited largely comparable transcriptional patterns, identifying CD160 as the only differentially expressed gene. Their analysis, however, was limited to 96 genes, whereas our transcriptomic dataset comprised 15,919 genes, which accounts for the absence of overlap between the studies. They also described increased proliferation and longer telomeres in IL21-expanded NK cells. In our work, although IL21-expanded NK cells displayed a more proliferative phenotype, we did not detect upregulation of telomerase reverse transcriptase (TERT) or other genes involved in telomere maintenance. Instead, the reduced expression of cytokines and cytokine receptors linked to differentiation may help explain their enhanced proliferative behavior. Furthermore, the similar expression of cytotoxicity-related receptors observed in our transcriptomic analysis is consistent with flow cytometry data and functional assays, all of which showed no significant differences in cytotoxic potential between IL21- and IL15-expanded NK cells.

Overall, PBMC- and CD45RA+-derived NKAE cells exhibited very similar transcriptional profiles, indicating that stimulation of either cell source generates NKAE populations with comparable phenotypes. This was supported by flow cytometric assessment of NK receptor expression. Nonetheless, among IL21-stimulated cells, PBMC-derived NKAE populations showed downregulation of genes within the hematopoietic cell lineage pathway, suggesting a more proliferative phenotype than NKAE cells generated from CD45RA+ cells. These transcriptomic findings align with our culture data, in which PBMC-derived NKAE cells displayed greater expansion than those obtained from CD45RA+ cells.

After determining the optimal culture medium and NK-cell source, we translated the protocol into a GMP-compliant setting and produced clinical-grade NKAE cells. Two manufacturing runs were carried out in the CliniMACS Prodigy system, coculturing purified CD56+ cells with either irradiated K562mbIL15 or K562mbIL21 feeder cells. In clinical production, two considerations are essential: (1) minimizing manufacturing time to allow timely infusion, and (2) reducing residual T cells to mitigate the risk of graft-versus-host reactions. For these reasons, purified CD56+ cells were selected as the starting population. Both feeder systems yielded large numbers of activated, highly cytotoxic NKAE cells that fulfilled all release criteria established by the Spanish Regulatory Agency. However, cultures with K562mbIL21 produced a 2.7-fold higher NK-cell expansion and generated NKAE cells with stronger cytolytic activity against K562 targets than those expanded with K562mbIL15. These observations mirror our small-scale results and suggest that K562mbIL21 is a more effective aAPC. Still, since only a single large-scale GMP run per condition was performed with two donors, interdonor variability may have contributed to the differences observed.

Earlier clinical trials by our group relied on manual PBMC coculture with irradiated K562mbIL15 in IL-2 and AB-serum–supplemented RPMI [32], yielding lower total cell numbers, NK-cell counts, and NK-cell purity ($639.78 \times 10^6 \pm 435.81$; $515.23 \times 10^6 \pm 345.03$; and $79.93\% \pm 17.43\%$, respectively) compared with the present work. Collectively, our data indicate that using purified CD56+ cells, K562mbIL21 feeder cells, TexMACS medium, and the CliniMACS Prodigy platform offers a substantially improved approach for generating clinical-grade NKAE cells.

In conclusion, we established an optimized strategy for expanding large quantities of fully functional NK cells across different cell sources, culture conditions, and aAPCs, and demonstrated that this system is scalable using a semi-automated, closed GMP platform. The resulting NKAE cells are suitable for direct clinical infusion or cryopreservation and represent a robust foundation for future NK-based therapeutic applications, including combination approaches such as BiKEs or CAR-engineered NK cells.

Materials and Methods

Peripheral blood mononuclear cells (PBMCs) were isolated from buffy coats of healthy volunteers using Ficoll–Paque density-gradient centrifugation. To obtain CD45RA-positive fractions, magnetic enrichment was performed with CD45RA microbeads, and the AutoMACS device was used following the manufacturer's "Possel" program. In some instances, these $CD45RA^+$ cells, typically discarded during haploidentical transplantation, were acquired from the Hematology Service at Hospital La Paz with written informed consent, in line with the

Declaration of Helsinki and the approval of the La Paz University Hospital Ethics Committee (protocol 4917). The study was conducted as part of a clinical trial registered under EudraCT 2016-003578-42. Buffy coats were provided by the Transfusion Centre of Comunidad de Madrid, with all donors meeting Spanish regulatory standards for the safe collection, storage, and handling of human cells and tissues.

Artificial antigen-presenting cells, specifically K562mbIL15 and K562mbIL21, were generously provided by Prof. Campana (National University Hospital, Singapore) and Prof. Lee (Nationwide Children's Hospital, Ohio, USA), respectively. Prior to coculture with NK cells, these aAPCs were irradiated at 100 Gy to prevent proliferation.

For the evaluation of optimal culture conditions, PBMCs were cocultured with irradiated K562mbIL15 cells at a ratio of 1:1.5 in one of four growth media: RPMI-1640, SCGM, NK MACS, or TexMACS GMP. All media were supplemented with 10% human AB serum and IL-2, initially at 10 IU/mL for the first week and increased to 100 IU/mL for subsequent days. Fresh medium was added every 48 hours to maintain a target density of one to two million cells per milliliter. To explore the potential of $CD45RA^+$ cells as a source for NKAE cells, PBMCs or $CD45RA^+$ fractions derived from mobilized or non-mobilized apheresis were cultured under similar conditions with irradiated K562mbIL15. To further determine the best combination of NK cell source and aAPC, PBMCs or $CD45RA^+$ cells were also cocultured with either K562mbIL15 or K562mbIL21 in TexMACS medium.

The expansion of total cells and NK cells, as well as the composition of lymphocyte subsets and cell viability, was monitored weekly using flow cytometry. For phenotypic analyses, a Navios flow cytometer was employed with specific conjugated antibodies, allowing the identification of T cells ($CD45^+CD3^+CD56^-$), B cells ($CD45^+CD19^+/CD20^+$), NKT cells ($CD45^+CD3^+CD56^+$), and NK cells ($CD45^+CD56^+CD3^-$), with NK cells further subdivided into CD56^dimCD16$^+$ and CD56^brightCD16$^-$ subsets. Functional receptors on NK cells were also assessed, and data analysis was conducted using FlowJo v10.0.7 software.

The cytotoxic activity of NKAE cells was measured between days 13 and 20 of culture using conventional 4-hour Europium-TDA release assays. Target cell lines included K562, Jurkat, A673, RH30, and LAN-1, with all cell lines cultured according to standard protocols and regularly tested for mycoplasma contamination. RH30 cells were kindly provided by Dr. Roma (Vall D'Hebron Institute of Research). Cytotoxicity was quantified as the percentage of specific release, calculated by normalizing experimental release against spontaneous and maximum release values.

To investigate transcriptomic changes, NK cells from two representative donors were collected before and after expansion. RNA was extracted using the RNeasy Mini Kit, with residual genomic DNA removed by DNase I digestion. RNA concentration, purity, and integrity were assessed using Qubit fluorometry, Nanodrop spectrophotometry, and TapeStation electrophoresis, respectively. Libraries were prepared with the TruSeq Stranded mRNA Library Prep Kit and sequenced on the NovaSeq 6000 platform with paired-end 100 bp reads, generating at least 25 million high-quality reads per sample.

RNA sequencing analysis of NK cells

The sequencing reads obtained from NK cells were aligned to the human genome reference hg19 using HISAT2. Transcript reconstruction and quantification were performed with StringTie, and differential gene expression between experimental conditions was analyzed using edgeR. Genes were considered differentially expressed when they showed a log fold change of at least 2 and a false discovery rate below 0.05. Heatmaps were generated for genes with a minimum expression of one count per million in more than one sample. Functional enrichment analysis was conducted with the clusterProfiler package, employing the enrichKEGG function to identify relevant pathways.

Manufacturing of clinical-grade NKAE cells

To accelerate the production of clinical-grade NKAE cells with maximal NK purity and minimal T cell contamination, $CD56^+$ cells were isolated before expansion. This ex vivo immunomagnetic purification involved sequential CD3 depletion followed by CD56 selection. The activation and expansion process was carried out using the CliniMACS Prodigy system with the T cell transduction (TCT) protocol and CliniMACS T520 tubing set. On day 0, cocultures were initiated with 2–2.5 × 10^6 NK cells and 4 × 10^7 irradiated K562mbIL15 or K562mbIL21 cells in 70 mL of GMP-grade TexMACS medium supplemented with 5% human AB serum and 100 IU/mL IL-2. During the first week, cultures were maintained under static conditions at 37 °C with 5% CO_2. Agitation was introduced on day 7, along with the addition of 70 mL of fresh medium, and expansion continued until day 14. Process monitoring included cell counts, viability assessment, flow cytometric analysis of $CD56^+/CD3^-$ content,

mycoplasma testing, and sterility checks at day 7. Final products were collected automatically in a sterile bag containing 0.9% sodium chloride and 0.5% human serum albumin. Quality control at the end of expansion encompassed total cell counts, viability, immunophenotyping of NK and T cell subsets, cytotoxicity assays against K562 cells, Gram staining, endotoxin quantification, assessment of residual aAPC by qPCR, mycoplasma testing, and sterility evaluation.

Analysis of cell count, viability, and NK cell purity

NKAE cells were enumerated using a CELL-DYN Emerald hematology analyzer, and their viability, surface phenotype, and activation markers were assessed by flow cytometry following previously described protocols.

Cytotoxicity

The functional activity of the manufactured NKAE cells was evaluated through conventional Europium-TDA assays against K562 target cells, using effector-to-target ratios of 8:1, 4:1, 2:1, and 1:1.

Microbiological tests

Expanded NKAE cell products were subjected to sterility testing in accordance with the European Pharmacopeia (Eu Ph 2.6.21). Conventional microbiological techniques were performed by the Clinical Microbiology and Parasitology Service of HULP, involving inoculation into specific culture media and monitoring for microbial growth over several days.

Analyses of non-cellular impurities

The presence of non-cellular contaminants was assessed following EuPh guidelines for endotoxins (Chapter 2.6.14) and mycoplasma (Chapters 2.6.21 and 2.6.7). Mycoplasma DNA was detected using a qPCR system with a DNA-binding dye, and endotoxin levels in the final products were measured with the Endosafe-PTS system (Charles River).

Analysis of cellular impurities

Because the aAPCs used for NK cell expansion are derived from tumor cell lines, it was essential to ensure the absence of residual K562mbIL15 or K562mbIL21 cells in the final NKAE product. Both aAPC lines contain the BCR/ABL fusion gene, and residual contamination was assessed by real-time PCR targeting the Mbcr transcript.

Genetic tests

At the conclusion of the manufacturing process, the expression of the oncogenes c-Myc and telomerase reverse transcriptase (TERT) was evaluated by qRT-PCR. Total RNA was extracted with the RNeasy kit and reverse transcribed using SuperScript IV. Quantitative PCR was performed on an ABI Prism 7900HT system using TaqMan probes, with GUSβ serving as the endogenous control. Reactions were run in triplicate, and relative gene expression was calculated using normalized GUSβ levels. To rule out chromosomal abnormalities, comparative genomic hybridization (CGH) was conducted. Genomic DNA from NKAE products was isolated and hybridized with male reference DNA on a 60K oligonucleotide CGH-SNP array. Data analysis utilized Agilent CGH analytics software with the ADAM-2 algorithm, using a sensitivity threshold of 6.0 and a 0.5 Mb window. Copy number alterations were defined by the presence of at least five consecutive altered probes, mapped to the GRCh37 (hg19) human genome assembly.

Statistical analysis

All data were analyzed using GraphPad Prism software and are presented as mean ± standard error of the mean (SEM). To determine whether datasets followed a normal distribution, Kolmogorov–Smirnov, D'Agostino–Pearson, and Shapiro–Wilk tests were applied. For data that did not meet normality assumptions, non-parametric methods were employed. Paired two-tailed Student's t-tests were used for comparisons between conditions within the same donor. When analyzing three or more groups, one-way ANOVA was conducted, accompanied by Dunn's post hoc tests for pairwise comparisons across all groups. For experiments involving two independent variables, two-way ANOVA with Bonferroni post hoc correction was applied to evaluate differences between replicates. A threshold of $p < 0.05$ was considered indicative of statistical significance.

Conclusion

This study established an optimized approach for expanding NKAE cells by testing four distinct culture media (RPMI, SCGM, TexMACS, and NK MACS), two NK cell sources (PBMCs and CD45RA$^+$ cells), and two irradiated aAPC types (K562mbIL15 and K562mbIL21). TexMACS emerged as the most effective medium for supporting NK cell growth. While CD45RA$^+$ cells from non-mobilized apheresis could be used for NKAE production, PBMCs consistently produced higher yields of purified NKAE cells. Expansion using K562mbIL21 as aAPC provided superior NK cell proliferation and reduced T cell contamination, independent of the NK cell source. NKAE cells generated from any combination of cell source and aAPC demonstrated robust cytotoxic activity against various tumor lines, including sarcoma, T-ALL, CML, neuroblastoma, and rhabdomyosarcoma. Furthermore, the protocol was successfully scaled to clinical-grade production using the CliniMACS Prodigy system. By purifying CD56$^+$ cells prior to expansion and culturing them with irradiated K562mbIL15 or K562mbIL21, large numbers of NKAE cells with high purity and minimal T cell contamination were produced within 14 days. Comprehensive quality control confirmed that the final products met regulatory standards, demonstrating their readiness for clinical application. This platform offers a reliable method for generating NKAE cells suitable for direct patient infusion, cryopreservation, or further enhancement for advanced NK cell therapies, such as CAR or BiKe modification.

Acknowledgments: None

Conflict of Interest: None

Financial Support: This work was supported by the National Health Service of Spain, Instituto de Salud Carlos III (ISCIII), FONDOS FEDER grant (FIS) PI18/01301 to Pérez-Martínez A, CRIS Foundation to Beat Cancer to Escudero A, Fernández A; Navarro A, Mirones I, and Fundación Mari Paz Jiménez Casado and La Sonrisa de Álex to Vela M.

Ethics Statement: None

References

1. Shimasaki N, Jain A, Campana D. NK cells for cancer immunotherapy. Nat Rev Drug Discov. 2020;19(3):200-18.
2. Miller JS, Soignier Y, Panoskaltsis-Mortari A, McNearney SA, Yun GH, Fautsch SK, et al. Successful adoptive transfer and in vivo expansion of human haploidentical NK cells in patients with cancer. Blood. 2005;105(8):3051-7.
3. Terme M, Ullrich E, Delahaye NF, Chaput N, Zitvogel L. Natural killer cell–directed therapies: Moving from unexpected results to successful strategies. Nat Immunol. 2008;9(5):486-94.
4. Cella M, Otero K, Colonna M. Expansion of human NK-22 cells with IL-7, IL-2, and IL-1β reveals intrinsic functional plasticity. Proc Natl Acad Sci U S A. 2010;107(24):10961-6.
5. Koehl U, Sorensen J, Esser R, Zimmermann S, Gruttner HP, Tonn T, et al. IL-2 activated NK cell immunotherapy… Blood Cells Mol Dis. 2004;33(3):261-6.
6. Son YI, Dallal RM, Mailliard RB, Egawa S, Jonak ZL, Lotze MT. IL-18 synergizes with IL-2 to enhance NK activity. Cancer Res. 2001;61(3):884-8.
7. Pérez-Martínez A, Fernández L, Valentín J, Martínez-Romera I, Corral MD, Ramírez M, et al. IL-15–stimulated NK infusion after haplo-HSCT. Cytotherapy. 2015;17(11):1594-603.
8. Hosseini E, Ghasemzadeh M, Kamalizad M, Schwarer AP. Ex vivo expansion of CD3-depleted cord blood MNCs… Stem Cell Res. 2017;19(1):148-55.
9. Masuyama J, Murakami T, Iwamoto S, Fujita S. NK expansion with anti-CD3/CD52. Cytotherapy. 2016;18(1):80-90.
10. Lee HR, Son CH, Koh EK, Bae JH, Kang CD, Yang K, et al. Expansion of cytotoxic NK cells using irradiated PBMCs and anti-CD16. Sci Rep. 2017;7(1):1-13.
11. Fujisaki H, Kakuda H, Shimasaki N, Imai C, Ma J, Lockey T, et al. Expansion of highly cytotoxic NK cells. Cancer Res. 2009;69(9):4010-7.
12. Wang X, Lee DA, Wang Y, Wang L, Yao Y, Lin Z, et al. Membrane-bound IL-21 and CD137L induce NK cells. Clin Exp Immunol. 2013;172(1):104-12.

13. Granzin M, Wagner J, Köhl U, Cerwenka A, Huppert V, Ullrich E. Shaping NK antitumor activity by ex vivo cultivation. Front Immunol. 2017;8:458.
14. Cho D, Shook DR, Shimasaki N, Chang YH, Fujisaki H, Campana D. Cytotoxicity of activated NK cells against pediatric solid tumors. Clin Cancer Res. 2010;16(15):3901-9.
15. Gong W, Xiao W, Hu M, Weng X, Qian L, Pan X, et al. NK expansion using K562-MICA/4-1BBL/IL-15. Tissue Antigens. 2010;76(6):467-75.
16. Apel M, Brüning M, Granzin M, Essl M, Stuth J, Blaschke J, et al. Integrated clinical-scale manufacturing system… Chem-Ing-Tech. 2013;85(1-2):103-10.
17. Oberschmidt O, Morgan M, Huppert V, Kessler J, Gardlowski T, Matthies N, et al. Automated NK separation & CAR engineering. Hum Gene Ther Methods. 2019;13(3):102-20.
18. Granzin M, Soltenborn S, Müller S, Kollet J, Berg M, Cerwenka A, et al. Fully automated expansion of NK cells. Cytotherapy. 2015;17(5):621-32.
19. Klöß S, Oberschmidt O, Morgan M, Dahlke J, Arseniev L, Huppert V, et al. Optimization of NK manufacturing; IL-21 with autologous feeders; anti-CD123-CAR NK. Hum Gene Ther. 2017;28(10):897-913.
20. Triplett BM, Shook DR, Eldridge P, Li Y, Kang G, Dallas M, et al. Rapid memory T-cell reconstitution… Bone Marrow Transplant. 2015;50(7):968-77.
21. Sisinni L, Gasior M, de Paz R, Querol S, Bueno D, Fernández L, et al. High incidence of HHV-6 encephalitis after naïve T-cell–depleted grafts. Biol Blood Marrow Transplant. 2018;24(11):2316-23.
22. Mamcarz E, Madden R, Qudeimat A, Srinivasan A, Talleur A, Sharma A, et al. Improved survival in T-cell depleted haplo-HCT. Bone Marrow Transplant. 2020;55(5):929-38.
23. Maschan M, Blagov S, Shelikhova L, Shekhovtsova Z, Balashov D, Starichkova J, et al. Low-dose donor memory T-cell infusion… Bone Marrow Transplant. 2018;53(3):264-73.
24. Geller MA, Miller JS. Use of allogeneic NK cells for cancer immunotherapy. Immunotherapy. 2011;3(12):1445-59.
25. Stern M, Passweg JR, Meyer-Monard S, Esser R, Tonn T, Soerensen J, et al. Pre-emptive immunotherapy with purified natural killer cells after haploidentical SCT: A prospective phase II study. Bone Marrow Transplant. 2013;48(3):433–8.
26. Barkholt L, Alici E, Conrad R, Sutlu T, Gilljam M, Stellan B, et al. Safety analysis of ex vivo-expanded NK and NK-like T cells administered to cancer patients: A phase I study. Immunotherapy. 2009;1(5):753-64.
27. Vela M, Corral D, Carrasco P, Fernández L, Valentín J, González B, et al. Haploidentical IL-15/41BBL–expanded NK cells after salvage chemotherapy in children with leukemia. Cancer Lett. 2018;422(1):107–17.
28. Bachanova V, Burns LJ, McKenna DH, Curtsinger J, Panoskaltsis-Mortari A, Lindgren BR, et al. Allogeneic NK cells for refractory lymphoma. Cancer Immunol Immunother. 2010;59(11):1739–44.
29. Curti A, Ruggeri L, D'Addio A, Bontadini A, Dan E, Motta MR, et al. Transfer of alloreactive haploidentical NK cells in elderly AML patients. Blood. 2011;118(12):3273–9.
30. Iliopoulou EG, Kountourakis P, Karamouzis MV, Doufexis D, Ardavanis A, Baxevanis CN, et al. Allogeneic NK infusion in NSCLC: Phase I trial. Cancer Immunol Immunother. 2010;59(12):1781–9.
31. Szmania S, Lapteva N, Garg T, Greenway A, Lingo J, Nair B, et al. Ex vivo-expanded NK cells in relapsed multiple myeloma. J Immunother. 2015;38(1):24–36.
32. Fernández L, Leivas A, Valentín J, Escudero A, Corral D, de Paz R, et al. Manufacture of IL-15–stimulated NK products. Transfusion. 2018;58(6):1340–7.
33. Vasu RS, Berg M, Davidson-Moncada J, Tian X, Cullis H, Childs RW. Expansion of $CD56^+$ NK cells from cryopreserved cord blood. Cytotherapy. 2015;17(11):1582–93.
34. Kloess S, Kretschmer A, Stahl L, Fricke S, Koehl U. CAR-expressing NK cells for cancer retargeting. Transfus Med Hemother. 2019;46(1):4–13.
35. Wagner J, Pfannenstiel V, Waldmann A, Bergs JWJ, Brill B, Huenecke S, et al. IL-15 + IL-21 NK expansion improves cytotoxicity. Front Immunol. 2017;8:676.
36. Kweon S, Phan MTT, Chun S, Yu HB, Kim J, Kim S, et al. Expansion of human NK cells using OX40L-K562 and IL-21. Front Immunol. 2019;10:879.
37. Cho D, Campana D. Expansion and activation of NK cells for immunotherapy. Korean J Lab Med. 2009;29(2):89–96.

38. Talleur A, Ying L, Salem A, Aksay S, Qudeimat A, Srinivasan A, et al. Haploidentical CD45RA− donor lymphocyte infusions: feasibility & benefit. Biol Blood Marrow Transplant. 2020;26(Suppl 3):S268.
39. Saraceni F, Shem-Tov N, Olivieri A, Nagler A. Mobilized PB grafts: Immunological perspective. Bone Marrow Transplant. 2015;50(7):886–91.
40. Su YC, Li SC, Hsu CK, Yu CC, Lin TJ, Lee CY, et al. G-CSF downregulates NK cytotoxicity in SCT donors. Bone Marrow Transplant. 2012;47(1):73–81.
41. Wong PPC, Kariminia A, Jones D, Eaves CJ, Foley R, Ivison S, et al. Plerixafor mobilizes CD56bright NK cells. Blood. 2018;131(25):2859–63.
42. Denman CJ, Senyukov VV, Somanchi SS, Phatarpekar PV, Kopp LM, Johnson JL, et al. Membrane-bound IL-21 sustains NK proliferation ex vivo. PLoS One. 2012;7(1):e30264.
43. Un PK, Ping J, Sabatino M, Feng J, Civini S, Khuu H, et al. Gene expression of expanded vs. fresh NK cells. J Immunother. 2010;33(9):945–55.